



# Mass Spectrometric Analysis of Urine from COVID-19 Patients for Detection of SARS-CoV-2 Viral Antigen and to Study Host Response

Sandip Chavan,<sup>¶</sup> Kiran K. Mangalparthi,<sup>¶</sup> Smrita Singh, Santosh Renuse, Patrick M. Vanderboom, Anil Kumar Madugundu, Rohit Budhreja, Kathrine McAulay, Thomas E. Grys, Andrew D. Rule, Mariam P. Alexander, John C. O'Horo, Andrew D. Badley, and Akhilesh Pandey\*



Cite This: <https://doi.org/10.1021/acs.jproteome.1c00391>



Read Online

ACCESS |



Metrics & More



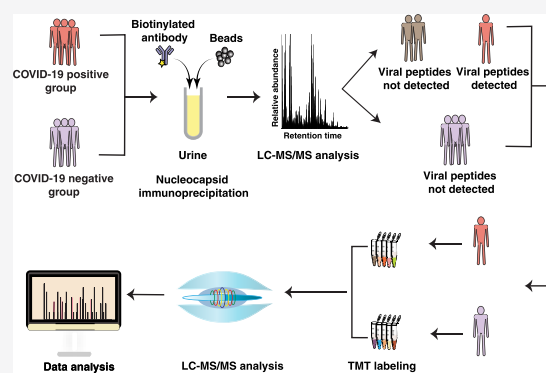
Article Recommendations



Supporting Information

**ABSTRACT:** SARS-CoV-2 infection has become a major public health burden and affects many organs including lungs, kidneys, the liver, and the brain. Although the virus is readily detected and diagnosed using nasopharyngeal swabs by reverse transcriptase polymerase chain reaction (RT-PCR), detection of its presence in body fluids is fraught with difficulties. A number of published studies have failed to detect viral RNA by RT-PCR methods in urine. Although microbial identification in clinical microbiology using mass spectrometry is undertaken after culture, here we undertook a mass spectrometry-based approach that employed an enrichment step to capture and detect SARS-CoV-2 nucleocapsid protein directly from urine of COVID-19 patients without any culture. We detected SARS-CoV-2 nucleocapsid protein-derived peptides from 13 out of 39 urine samples. Further, a subset of COVID-19 positive and COVID-19 negative urine samples validated by mass spectrometry were used for the quantitative proteomics analysis. Proteins with increased abundance in urine of SARS-CoV-2 positive individuals were enriched in the acute phase response, regulation of complement system, and immune response. Notably, a number of renal proteins such as podocin (NPHS2), an amino acid transporter (SLC36A2), and sodium/glucose cotransporter 5 (SLC5A10), which are intimately involved in normal kidney function, were decreased in the urine of COVID-19 patients. Overall, the detection of viral antigens in urine using mass spectrometry and alterations of the urinary proteome could provide insights into understanding the pathogenesis of COVID-19.

**KEYWORDS:** SARS-CoV-2, COVID-19, coronavirus, urine, mass spectrometry, quantitative proteomic analysis



## INTRODUCTION

The coronavirus SARS-CoV-2 (severe acute respiratory syndrome coronavirus 2), responsible for COVID-19, has already infected millions worldwide.<sup>1</sup> The detection of SARS-CoV-2 virus by reverse transcriptase polymerase chain reaction (RT-PCR) using nasopharyngeal or oropharyngeal swabs has been used to confirm the clinical diagnosis of COVID-19. The virus has also been detected in saliva and fecal samples,<sup>2,3</sup> although results from urine have been less promising. The large majority of studies on COVID-19 have not been able to detect SARS-CoV-2 RNA in urine even by RT-PCR,<sup>3,4</sup> although some studies have reported detecting it in a small number of samples.<sup>5–7</sup> The reasons for failure to detect the virus in urine could be due to the lack of viral particles or the labile nature of RNA.

SARS-CoV-2 infects cells via interaction between the spike (S) protein of the virus and angiotensin-converting enzyme 2 (ACE2) receptor present on the cell surface.<sup>8,9</sup> The ACE2 receptor is abundantly present on the cells of lungs, gastrointestinal tract, heart, brain, liver, and kidneys.<sup>10</sup> It has been shown that SARS-CoV-2 causes acute cardiac injury, heart

failure and cardiac arrhythmias,<sup>11,12</sup> meningitis, cranial nerve deficits, encephalopathy,<sup>13</sup> abnormal liver function,<sup>14,15</sup> and acute renal injury<sup>16</sup> in critically ill patients. Upon encounter of SARS-CoV-2 infection, the host immune response aims to defend against and clear the infection by using both innate and adaptive immunity. Thus far, several studies have been performed mainly in serum, plasma, and nasopharyngeal swabs to identify the components involved in host immune response.

A large fraction of proteins in the urine are shed from the kidneys;<sup>17</sup> thus, any change in physiology of an individual could potentially be reflected in the protein composition of urine. Recent MS-based proteomics studies have examined urine

Received: May 10, 2021



samples of COVID-19 patients for evaluating the host immune response to SARS-CoV-2 infection.<sup>18,19</sup> In one study, upregulation of proteins associated with complement activation and hypoxia and downregulation of proteins associated with platelet degranulation was observed in urine of patients with severe COVID-19.<sup>18</sup> Another study showed a decreased expression of proteins involved in the immune system, complement activation, and chemokine signaling, which suggest immunosuppression in the early stages with an increase in the later stages of COVID-19.<sup>19</sup> Although significant achievements have been made in this area, the pathogenesis of COVID-19 and the exact nature of immune responses that are elicited in those who are infected is still unclear. In this study, we used a mass-spectrometry-based approach to demonstrate the presence of SARS-CoV-2-derived antigens in the urine. We further performed a quantitative proteomics analysis of urine samples that tested positive for SARS-CoV-2 via mass spectrometry and control urine samples to investigate the host response.

## MATERIALS AND METHODS

Residual urine samples collected from 39 COVID-19 patients confirmed to be positive for the SARS-CoV-2 virus by RT-PCR testing of nasopharyngeal swabs were included. Eleven urine samples collected from patients confirmed to be negative for the SARS-CoV-2 virus by RT-PCR testing of nasopharyngeal swabs were used as controls. All samples were obtained with approval under the Mayo Clinic's Institution Review Board (IRB 20-005116 and IRB 20-003820).

### Immunocapture of Nucleocapsid Protein from Urine Samples

The collected urine samples were inactivated by heating at 70 °C (60 °C for samples collected from Mayo Clinic, Arizona) for 30 min. The inactivated urine samples (1 mL each) were then subjected to immunoprecipitation. The immunoprecipitation was carried out using a biotinylated antinucleocapsid antibody in the urine collected from 39 COVID-19 patients positive for SARS-CoV-2. In parallel, urine samples from 11 COVID-19 negative samples were processed. The SARS-CoV-2 nucleocapsid monoclonal antibody (Sino Biological Inc., Wayne, PA) was biotinylated using EZ-Link Sulfo-NHS-Biotin (Thermo Scientific, Waltham, MA) according to the manufacturer's instructions. Urine samples were diluted 2-fold with phosphate buffered saline (PBS) and incubated overnight at 4 °C with 1 μg of biotinylated antibody on a Thermomixer (Eppendorf, Hamburg, Germany) with rotation at 1400 rpm. Following incubation, 25 μL of streptavidin-coated magnetic beads (Dynabeads M-280 Streptavidin, Thermo Scientific, Waltham, MA) was added and the samples were incubated for an additional 30 min. The samples were then placed on a magnetic separator, and the settled magnetic beads were washed three times with PBS. After the last wash, the captured nucleocapsid protein was eluted with two successive additions of 25 μL of elution buffer (0.1% trifluoroacetic acid (TFA), 50% acetonitrile, and 0.002% Zwittergent 3–16 detergent (MilliPore Sigma)). The eluted nucleocapsid protein was neutralized with 150 μL of rapid digest buffer (Promega, Madison, WI).<sup>20</sup> Briefly, the protein samples were reconstituted in the rapid trypsin digestion buffer, and 0.5 μg of trypsin was added to each sample. The mixture was then incubated at 70 °C for 1 h. After digestion, peptides were desalted using C<sub>18</sub> and vacuum-dried, reconstituted, and subjected to LC-MS/MS analysis.

### Sample Preparation for Quantitative Proteomics Analysis

All urine samples were processed separately. A total of 1 mL of each urine sample from five positive and five negative patients was concentrated using a 3 kDa filter separately. A total of 100 μg of protein from each sample was used after a bicinchoninic acid (BCA) protein assay (Pierce Waltham, MA). The samples were then reduced using 5 mM dithiothreitol and alkylated using 10 mM iodoacetamide, followed by digestion using trypsin at a 1:20 enzyme to substrate ratio. The digested peptides were tandem mass tag (TMT) labeled as per the manufacturer's instructions. Briefly, peptides were dissolved in 50 mM TEABC (pH 8.0), and TMT reagents were added (dissolved in anhydrous acetonitrile) to the peptide. After incubation at room temperature for 1 h, the reaction was quenched with 5% hydroxylamine. All the labeled samples were pooled and subjected to basic pH reversed-phase fractionation, as described previously.<sup>21</sup> Briefly, TMT 10-plex labeled samples were pooled and dissolved in basic pH reversed phase chromatography (BRPLC) solvent A (5 mM TEABC, pH 8.5) and fractionated on a C<sub>18</sub> XBridge column (5 μm, 250 × 4.6 mm, Waters) using an increasing gradient of solvent B (5 mM TEABC, pH 8.5, 90% acetonitrile) on the UltiMate 3000 HPLC system (Thermo Fisher Scientific, Waltham, MA). The absorbance of eluted peptides was measured at 280 nm. The total run time was 120 min, and 96 fractions were collected, which were subsequently concatenated into 24 fractions. These fractions were then vacuum-dried.

### LC-MS/MS Analysis

The LC-MS/MS analysis of digested urine samples was carried out using the Ultimate 3000 RSLC nano system interfaced with an Orbitrap Fusion Lumos Tribrid mass spectrometer (Thermo Scientific, San Jose, CA). The peptides were preconcentrated on a trap column (PepMap C<sub>18</sub>, 2 cm × 100 μm, 100 Å, Thermo Scientific, San Jose, CA) at a flow rate of 20 μL/min using 0.1% formic acid (solvent A). These peptides were then separated on an analytical column (EasySpray 50 cm × 75 μm, C<sub>18</sub> 1.9 μm, 100 Å, Thermo Scientific, San Jose, CA) using a 300 nL/min flow rate and a linear gradient of 5 to 30% solvent B (100% ACN, 0.1% formic acid) over a 75 min gradient. The precursor ions were acquired at a resolution of 120 000 and the fragment ions at a resolution of 15 000 (at *m/z* 200) in the Orbitrap mass analyzer. The precursor ions were acquired in the range of 350–1700 *m/z*, and the fragmentation was carried out using a higher-energy collisional dissociation (HCD) method using a normalized collision energy (NCE) of 28 for discovery analysis of the immuno-enriched fractions and NCE of 35 for TMT-labeled fractions. The scans were arranged in a top-speed method with a 2 s cycle time between MS and MS/MS. Ion transfer capillary voltage was maintained at 2.0 kV. For internal mass calibration, a lock mass option was enabled with a polysiloxane ion (*m/z*, 445.120025) from ambient air.

The raw mass spectrometry data were searched using Sequest and Mascot through Proteome Discoverer 2.3.0.523 (Thermo Scientific, San Jose, CA) against a combined protein database of SARS-CoV-2 proteins, SARS-CoV proteins, common coronaviruses (OC43, HKU1, NL63, and L229E), and UniProt human protein database including common MS contaminants. The search parameters included trypsin as the enzyme with a maximum of two missed cleavages: N-terminal acetylation and oxidation at methionine as variable modifications. Raw files for TMT-labeled samples were searched with the Sequest search engine using the same databases as described above. In addition to the modifications described above, carbamidomethylation on

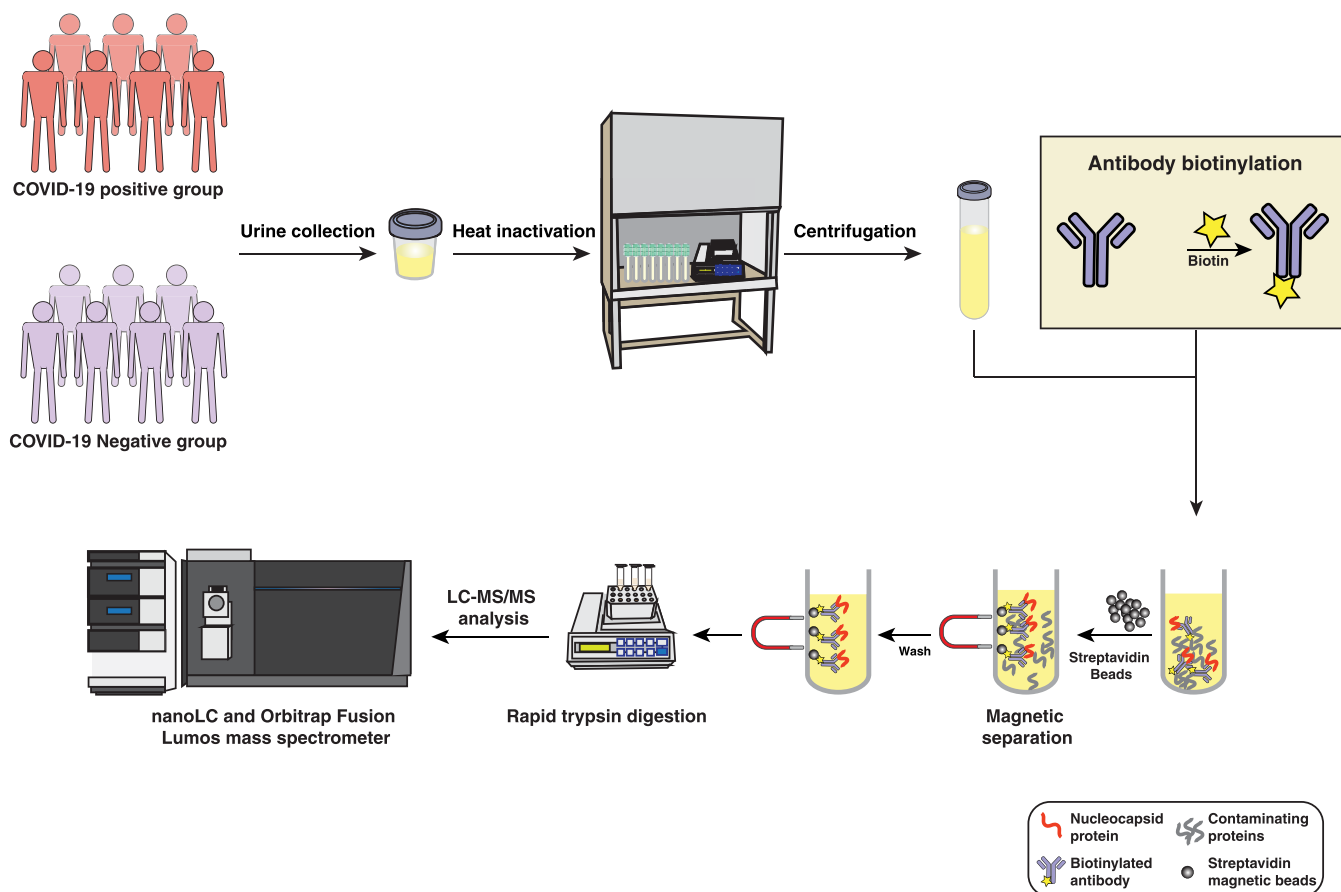


**Figure 1.** Experimental workflow for the detection of SARS-CoV-2 using mass spectrometry in urine samples. SARS-CoV-2 positive urine ( $n = 39$ ) and negative (control) urine ( $n = 11$ ) samples were centrifuged, inactivated, and subjected to immunoprecipitation (IP) of nucleocapsid protein using a biotinylated antinucleocapsid monoclonal antibody. Rapid trypsin digestion was carried out on IP eluate followed by  $C_{18}$  clean up and LC-MS/MS analysis.

cysteine as a fixed modification, TMT mass was specified as a fixed modification at the N-terminus and lysine. Precursor tolerance was set to 10 ppm and MS/MS tolerance to  $\pm 0.02$  Da. The false discovery rate was set to 1% at the peptide-spectrum matches (PSMs), peptide, and protein levels.

### Data Analysis

Statistical analysis was performed using the Perseus computational platform.<sup>22</sup> The abundance values from TMT channels were analyzed using two-sample student's  $t$  test to identify differentially abundant proteins in urine samples of SARS-CoV-2 patients. Unsupervised clustering of the differentially abundant proteins was performed using Perseus. Gene ontology enrichment analysis was performed using the DAVID Bioinformatics resource using a custom background.<sup>23</sup> A protein–protein interaction network was generated using the String web server.<sup>24</sup>

The mass spectrometry proteomics data have been deposited to the Proteome Xchange Consortium via the PRIDE partner repository with the data set identifier PXD024967.

## RESULTS

### Study Population

The study was approved by the Institutional Review Board at the Mayo Clinic. In all, we studied 39 patients who tested positive for SARS-CoV-2 via RT-PCR of nasopharyngeal swab samples. Random (not timed) urine samples obtained a median of 1 day (range 0–39 days) after testing positive were processed

individually. We also studied 11 controls that were selected from subjects who presented with symptoms but had a negative SARS-CoV-2 diagnostic test by RT-PCR. Their urine samples were obtained a median of zero days (range 0–24 days) after testing negative and were processed individually. The inactivated urine samples were further centrifuged to remove cells and particulate matter.

### Detection of Viral Antigens in Urine Using Immunoenrichment and LC-MS/MS

Urine samples from 39 COVID-19 patients and 11 negative controls were used for the detection of viral antigens. The overall workflow for the urine immunoprecipitation followed by mass spectrometry analysis used in the current study is outlined in Figure 1. Briefly, inactivated urine samples were incubated with biotinylated antibodies directed against viral nucleocapsid protein overnight to allow efficient capture of the antigen. The antigen–antibody complex was captured using streptavidin coupled beads, and the enriched viral nucleocapsid protein was eluted and digested using a rapid trypsin digestion protocol. The digested samples were then analyzed using an Orbitrap Lumos mass spectrometer.

LC-MS/MS analysis led to the detection of viral peptides in 13 out of 39 COVID-19 positive patient samples. Out of the 13 samples which were positive by immunoprecipitation-mass spectrometry (IP-MS), urine osmolality of the 12 COVID-19 urine antigen positive patients was  $402 \pm 124.90$  mOsm/kg compared to  $529 \pm 84.82$  mOsm/kg in the 23 COVID-19 urine

**Table 1. Baseline Characteristics and Laboratory Features of COVID-19 Positive Cases<sup>a</sup>**

characteristic	patients with SARS-CoV-2 antigens in urine (n = 12)	patients without SARS-CoV-2 antigens in urine (n = 23)
age >60 years	8 (66.7%)	9 (39.1%)
male	8 (66.7%)	11 (47.8%)
race		
white	8 (66.7%)	14 (60.9%)
African American	1 (8.3%)	4 (17.4%)
Asian	1 (8.3%)	3 (13%)
other	2 (16.7%)	2 (8.7%)
deceased	5 (41.7%)	2 (8.7%)
ventilator support	7 (58.3%)	5 (21.7%)
comorbidities		
hypertension	5 (41.7%)	10 (43.5%)
type 2 diabetes mellitus	2 (16.7%)	6 (26.1%)
cardiovascular disease	9 (75%)	11 (47.8%)
chronic lung disease	6 (50%)	1 (4.3%)
chronic kidney disease	2 (16.7%)	9 (39.1%)
liver disease	2 (16.7%)	6 (26.1%)
pneumonia/ARDS	11 (91.7%)	14 (60.9%)
acute kidney failure	4 (33.3%)	6 (26.1%)
acute on chronic kidney failure	2 (16.7%)	3 (13%)
signs and symptoms		
fever	6 (50%)	3 (13%)
cough	2 (16.7%)	9 (39.1%)
diarrhea	1 (8.3%)	5 (21.7%)
myalgia	3 (25%)	2 (8.7%)
hypoxemia	3 (25%)	4 (17.4%)
shock	4 (33.3%)	3 (13%)
laboratory features		
leukopenia (<4 × 10 <sup>9</sup> /L)	1 (8.3%)	0 (0%)
thrombocytopenia (<150 × 10 <sup>9</sup> /L)	5 (41.7%)	1 (4.3%)
elevated CRP (>10 mg/L)	12 (100%)	12 (52.2%)
elevated AST (>48 U/L)	5 (41.7%)	7 (30.4%)
elevated ALT (>55 U/L)	2 (16.7%)	4 (17.4%)
elevated total bilirubin (>1.2 mg/dL)	0 (0%)	2 (8.7%)
low serum albumin (<3.5 g/dL)	7 (58.3%)	7 (30.4%)
elevated serum creatinine (>1.21 mg/dL)	5 (41.7%)	6 (26.1%)
elevated BUN (>20 mg/dL)	6 (50%)	9 (39.1%)
prolonged PT (>14 s)	4 (33.3%)	3 (13%)
elevated urine protein (>14 mg/dL)	10 (83.3%)	13 (56.5%)

<sup>a</sup>ARDS, acute respiratory distress syndrome; CRP, C-reactive protein; AST, aspartate aminotransferase; ALT, alanine aminotransferase; BUN, blood urea nitrogen; PT, prothrombin time.

IP-MS negative patients (p-value = 0.07), suggesting urine concentration did not affect detection of the viral antigens. The demographic, clinical, and laboratory parameters are presented

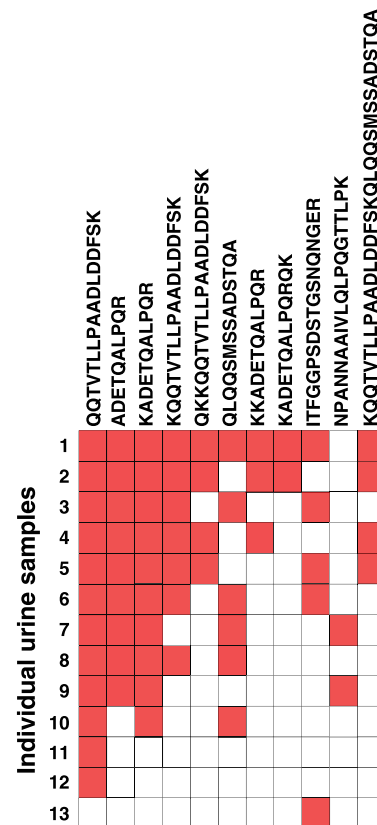


**Figure 2.** Summary of the LC-MS/MS analysis for the detection of peptides derived from SARS-CoV-2 nucleocapsid protein. Peptides identified in the urine samples are highlighted in red, while unfilled boxes represent peptides not detected in the indicated samples. Peptides derived from the nucleocapsid protein were not detected in any of the negative control urine samples.

in Table 1 for 35 out of 39 patients positive for SARS-CoV-2 by RT-PCR. The patient information for remaining patients was not available. Among these, the 12 patients positive for nucleocapsid peptides in urine were more likely to have chronic lung disease, fever, low platelets, elevated CRP, and higher mortality than the 23 patients without urine viral peptides (Table 1). Eleven different peptides from the nucleocapsid protein were identified from at least one positive urine sample. Of these, QQTVTLLPAADLDDFSK was identified from 12 samples, ADETQALPQR from nine samples, and KADETQALPQR from 10 samples. The heat map in Figure 2 depicts all the identified peptides from 13 samples. The identified peptides were mapped onto nucleocapsid protein, and representative spectra for four of the identified peptides from SARS-CoV-2 are shown in Figure 3. As expected, the viral proteins were not detected in the urine of any of the 11 COVID-19 negative samples.

#### Quantitative Proteomics Analysis of Urine from Individuals with COVID-19

Identification of SARS-CoV-2 viral antigens in urine indicates possible infection of several tissues and thus disease severity. Thus, urine can be a potential source of biomarkers to track the progression of disease and to monitor the host response. To better understand this, we also carried out mass spectrometry-based quantitative proteomics analysis using a multiplexing strategy. Urine from five SARS-CoV-2 individuals tested positive by mass spectrometry and five negative individuals was used for

A

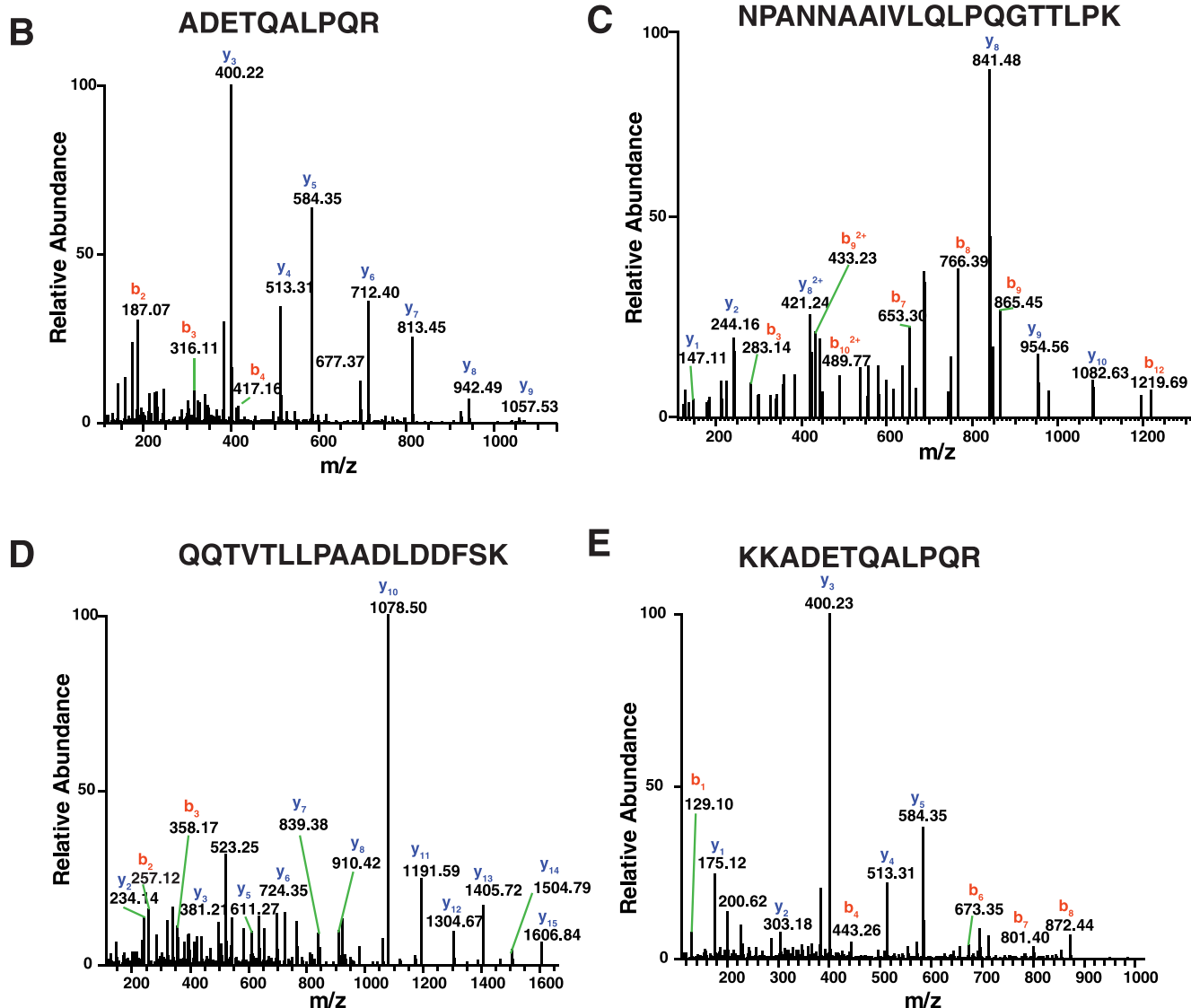
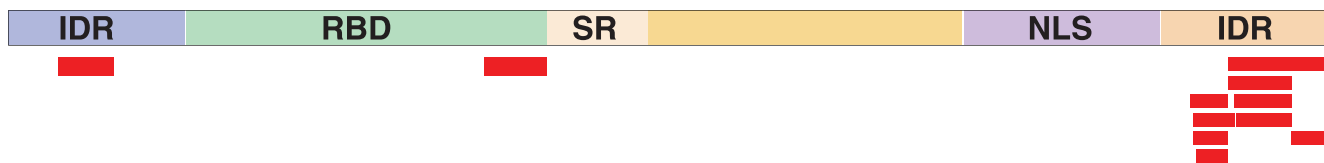


**Figure 3.** (A) Peptides identified in LC-MS/MS analysis of SARS-CoV-2 positive urine samples mapped onto nucleocapsid protein domains. RBD = RNA binding domain; SR = serine-arginine-rich; NLS = nuclear localization signal; IDR = intrinsically disordered region. Red block indicates the region of the respective regions of nucleocapsid protein identified by peptides in the LC-MS/MS analysis. Representative MS/MS spectra of the peptides (B) ADETQALPQR, (C) NPANNAIIVLQLPQGTTLPK, (D) QQTVTLLPAADLDDFSK, and (E) KKADETQALPQR identified from the LC-MS/MS analysis of SARS-CoV-2 positive urine samples.

this study. The five negative samples used for the quantitative analysis were also negative by IP-MS analysis. A total of 1 mL of each urine sample was concentrated using a 3 kDa filter followed by the digestion of proteins. After labeling the digests with TMT 10-plex reagents, the pooled sample was fractionated into 24 fractions and analyzed by LC-MS/MS.

LC-MS/MS analysis of 24 fractions resulted in the identification of 1488 proteins at 1% protein-level FDR (Table S1). To identify the proteins that were differentially abundant in the urine of SARS-CoV-2 individuals, we performed two sample student's *t* test on the log transformed abundance values of 1351 proteins quantified from all 10 samples. After applying a fold

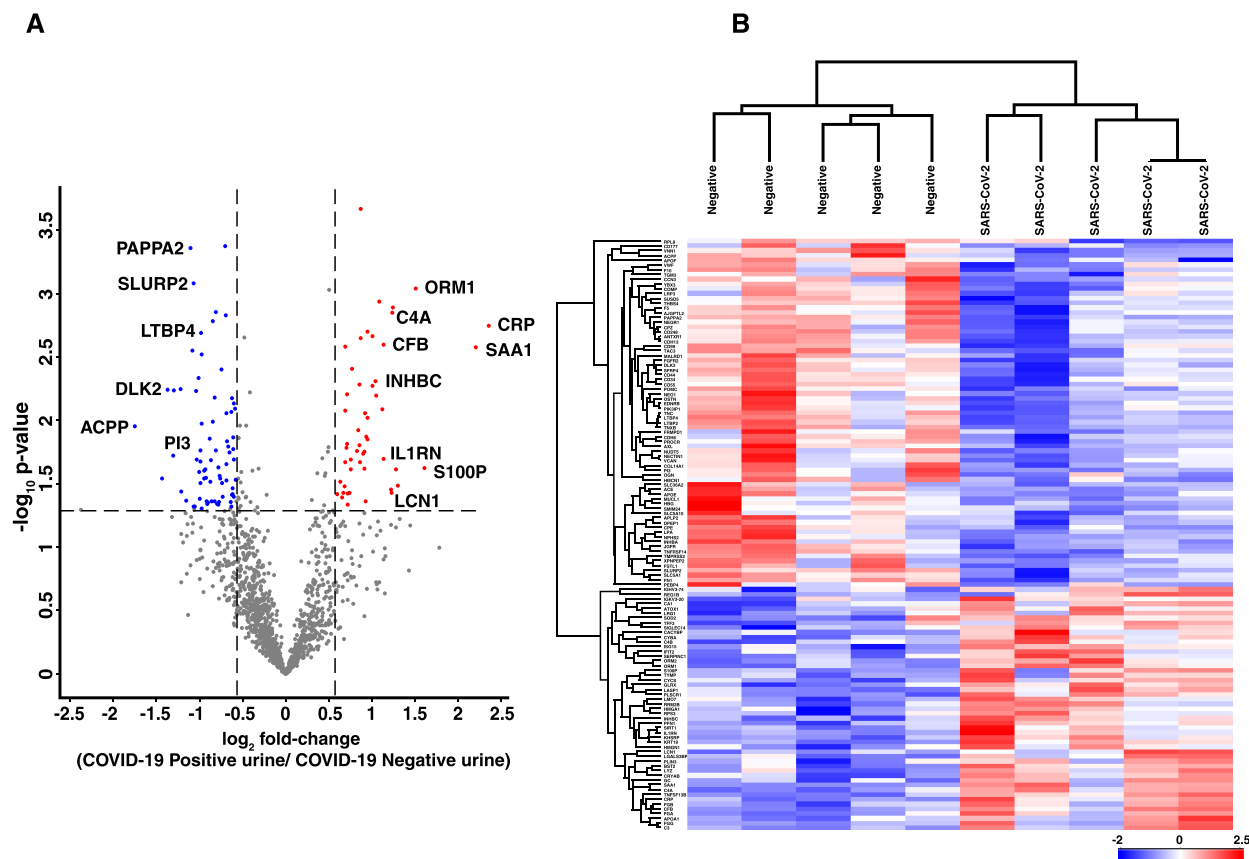


**Figure 4.** Quantitative analysis of urinary proteins from SARS-CoV-2 positive and negative individuals. (A) Volcano plot depicting the differentially abundant proteins in urine of SARS-CoV-2 positive individuals compared to negative controls. Statistical analysis was performed by two-sample *t* test, and proteins were filtered 1.5-fold and for *p* values < 0.05. (B) Unsupervised clustering of the differentially abundant proteins identified distinct clusters of protein abundance in SARS-CoV-2 positive and negative control individuals.

change cutoff of 1.5-fold and a *p* value < 0.05, we identified 112 proteins that were differentially abundant with 45 proteins at a higher level and 68 proteins at a lower level in the urine of COVID-19 infected individuals as compared to negative samples (Figure 4A and Table S2). Hierarchical clustering of the differentially abundant proteins clearly segregated SARS-CoV-2 infected individuals from the negative individuals (Figure 4B). These proteins probably indicate a host response signature in individuals infected by SARS-CoV-2. We next compared the differentially abundant proteins identified in our study with a recently published study on urine samples using a label-free proteomics strategy and found 39 of the 112 proteins in our list to be common, suggesting some overlap with the previous report.<sup>18</sup>

#### Functional Characterization of the Differentially Abundant Proteins

We next performed functional characterization of the differentially abundant proteins identified in this study. Using the DAVID resource, we found that the proteins with increased abundance in urine of SARS-CoV-2 positive individuals were involved in several biological processes such as the acute phase response, innate immune response, regulation of complement activation, and platelet activation (Fischer's exact test, *p* value < 0.05; Figure 5A and Table S3A). These results indicate activation of the immune components upon SARS-CoV-2 infection, which is consistent with the recently reported findings in the urine of severe COVID-19 cases.<sup>18,19</sup> Increased abundance of proteins involved in the regulation of the

complement system include complement C3, complement 4A, complement 4B, and complement factor B. Several proteins involved in the antiviral immune response were also increased in abundance in the urine of SARS-CoV-2 patients such as MX1, B2M, BST2, SAA1, IFIT2, ISG15, and PLS1 (Figure 5B). Molecular functions enriched among the proteins with increased abundance in urine include complement component C1q binding, serine type endopeptidase activity, and receptor binding (Figure 5C). Proteins with decreased abundance in the urine of SARS-CoV-2 patients were enriched in biological processes such as cell adhesion, extracellular matrix organization, and leukocyte migration (Table S3B). These proteins include VCAN, CAD13, DSC2, FINC, COMP, TENX, and SUSD5. Heparin binding, calcium ion binding, collagen binding, and extracellular matrix structural constituents were among the significantly enriched molecular function terms.

Apart from the systemic host response that is reflected in the urinary proteome, the proteins found in urine can also indicate renal pathology. In support of this, we observed a decreased abundance of several proteins in the urine of SARS-CoV-2 patients which are known to be enriched in kidney tissue. These proteins include NPHS2, DPEP1, XPNPEP2, SMIM24, SLC5A10, SLC47A1, and SLC36A2 (Figure 5D). NPHS2, podocin, is a podocyte marker located in the foot process of the podocyte cells. Podocin plays a critical role in the function of glomerular filtration, and defects in podocin are known to cause focal and segmental glomerulosclerosis (FSGS),<sup>25</sup> nephrotic syndrome,<sup>26</sup> and ultimately kidney failure.

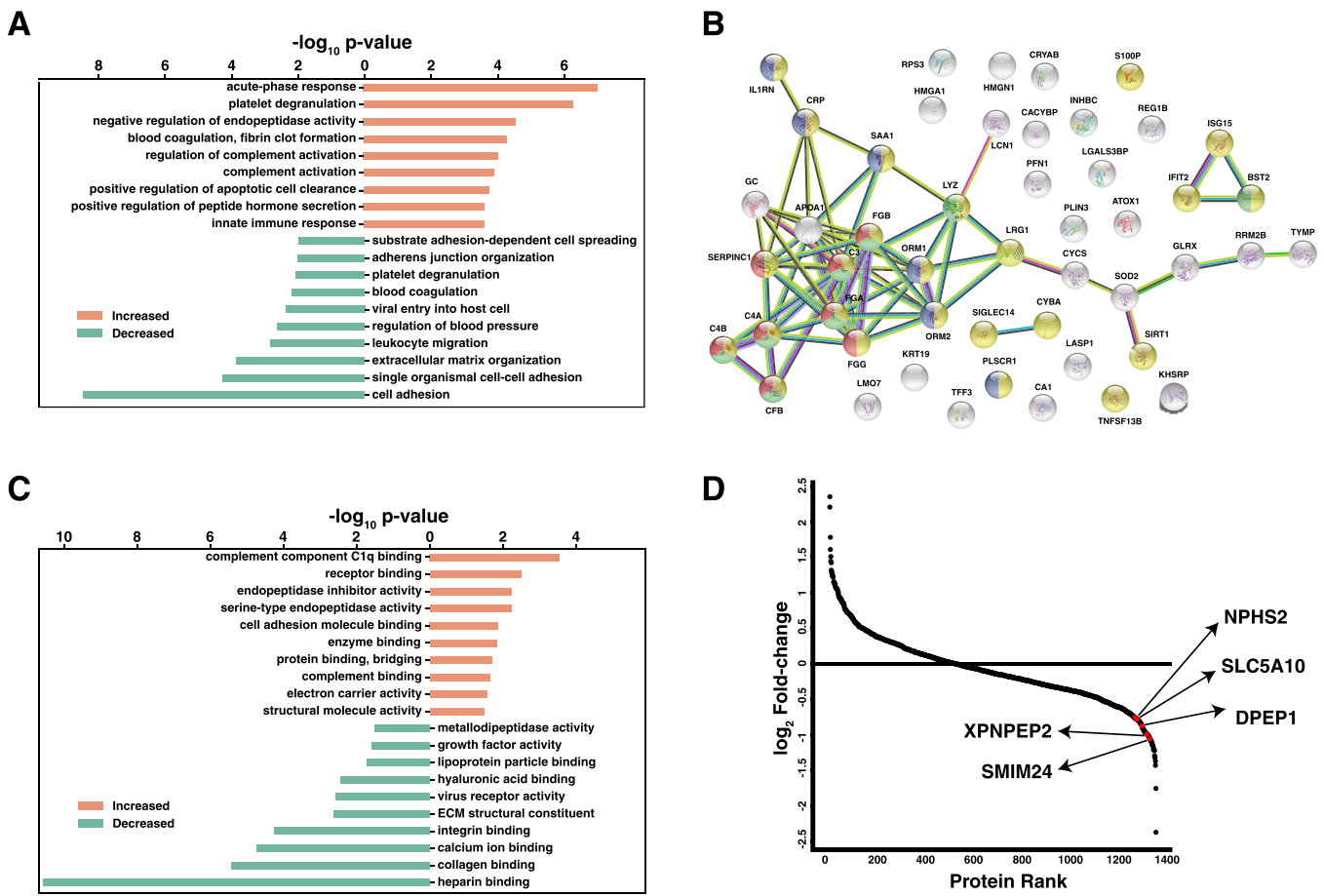


**Figure 5.** Functional characterization of the differentially abundant proteins. Gene ontology enrichment analysis of the differentially abundant proteins was performed by Fisher's exact test using the DAVID resource. (A) Enriched biological processes among the differentially abundant proteins. (B) Protein–protein interaction network highlighting the enrichment of proteins involved in immune responses among the overabundant proteins in the urine of SARS-CoV-2 positive individuals. Nodes with yellow color are involved in immune response. Nodes with red color belong to the complement system, and nodes with green color belong to the acute phase response. (C) Enriched molecular function terms among the differentially abundant proteins. (D) S-plot representation of the kidney tissue enriched proteins with decreased abundance in the urine of SARS-CoV-2 positive individuals.

XPNPEP2 has been identified as a key inactivator of bradykinin peptide, a potent vasodilator.<sup>27</sup> This protein is abundantly expressed in the heart, placenta, liver, small intestine, colon, lungs, and kidneys.<sup>28</sup> Previous studies have found an association of XPNPEP2 with angiotensin I-converting enzyme inhibitors (ACEi)-angioedema, in which decreased degradation of vasoactive peptides leads to a life-threatening adverse reaction.<sup>27,29,30</sup> Another protein, SLC36A2, is abundantly present in kidneys and muscles and known to be involved in the reabsorption of glycine, proline, and hydroxyproline in the kidney proximal tubule.<sup>31,32</sup> The mutation in the SLC36A2 gene leads to iminoglycinuria, in which the above-mentioned amino acids do not get absorbed by the kidneys, marked by excessive amount of these amino acids in urine.<sup>31</sup> Recently, it was shown that the SARS-Cov-2 virus causes dysfunction of the kidney proximal tubule in the COVID-19 patients.<sup>33</sup> Sodium/glucose cotransporter 5 (SLC5A10) is a transmembrane protein that belongs to the SLC5 gene family and is involved in active transport of monosaccharides such as mannose, glucose, galactose, and fructose.<sup>34</sup> This transporter is exclusively present in the kidney, where it mediates the reabsorption of these monosaccharides back into the blood from the glomerular filtrate.<sup>34,35</sup>

## DISCUSSION

RT-PCR is still the gold standard method for detecting the SARS-CoV-2 virus in nasopharyngeal samples. However, several studies have failed to detect SARS-CoV-2 in urine. In this study, we demonstrated the presence of SARS-CoV-2 viral antigen in the urine of patients with COVID-19 using mass spectrometry and characterized the urinary proteome to study the host response. To our knowledge, this is the first study describing the detection of viral antigens in urine samples from COVID-19 patients and enrichment of the nucleocapsid protein could be the crucial step in successfully detecting SARS-CoV-2 viral peptides. It has previously been shown that SARS-CoV nucleocapsid protein expression is increased during infection and is involved in the nuclear-import signal, virus replication, and RNA packaging.<sup>36</sup> A cell infected with SARS-CoV-2 contains several virions with each virion containing ~1000 nucleocapsid molecules.<sup>37</sup> It is also likely that the viral proteins are more stable than the viral RNA genome. Thus, using the latest LC-MS/MS instrumentation, nucleocapsid protein can be detected reliably in urine even when the viral load is low. However, further studies will be required to determine the clinical utility of urinary viral antigens as prognostic markers in COVID-19 patients. This study is especially relevant because under current clinical practice, microbial diagnosis from clinical

samples such as sputum, urine, and swabs using a mass spectrometry approach requires a culture of microbes to obtain a pure population of organisms. We foresee that immunopurification followed by mass spectrometry can become a viable alternative as a diagnostic tool in the future for identification of pathogens directly from such clinical specimens without culture, as this approach could potentially reduce the time for clinical diagnosis by 24–28 h.

Several recent studies have suggested that the renal dysfunction in SARS-CoV-2 is more likely the sequelae of indirect injury from cytokine storms, sepsis, and immune dysregulation as opposed to direct viral toxicity.<sup>38</sup> Recently, Braun et al. showed the presence of SARS-CoV-2 RNA in autopsy kidneys in patients with acute kidney injury which correlated with disease severity in these patients.<sup>39</sup> They were also able to isolate viable SARS-CoV-2 virus from one case.<sup>39</sup> Their findings support our data and the possible utility of early urinary testing for SARS-CoV-2 for predicting the risk of kidney injury in COVID-19. In this study, we identified a decreased abundance of several proteins involved in proximal tubule function and membrane transporter roles (SLC5A10, SLC47A1, and SLC36A2) which is supportive of proximal tubular dysfunction in SARS-CoV-2.<sup>35</sup> The actual mechanism of SARS-CoV-2 associated kidney injury is unclear. Ischemia and sepsis are possible mechanisms of acute kidney injury. Ischemia causes impaired and decreased expression of Na<sup>+</sup> transporter proteins,<sup>40–42</sup> suggesting that perhaps ischemia is one mechanism of SARS-CoV-2 associated acute kidney injury. The finding of increased abundance of complement Factor B with a decreased abundance of transporter proteins has been reported earlier in sepsis; this supports a recent hypothesis suggesting that SARS-CoV-2 associated renal injury might in fact be sepsis-associated kidney injury.<sup>43</sup> The downregulation of podocyte protein NPHS2 might also be associated with increased endocytic processes noted in COVID-19.

In conclusion, despite several failed attempts to detect SARS-CoV-2 in urine,<sup>3</sup> we showed for the first time the presence of SARS-CoV-2 viral peptides in urine. This study is a proof of principle study to demonstrate that we can indeed identify viral peptides in urine using mass spectrometry. The detection of viral peptides does not necessarily indicate the presence of viable virus particles in the urine as it could also indicate degraded viral proteins. However, a recent article has shown the infectivity of one urine sample from a SARS-CoV-2 individual to exert a cytopathic effect on the Vero-E6 cell line.<sup>5</sup> This indicates that intact viral particles can be present in the urine samples, and further studies using viral culture in a BSL-3 setting will be required to confirm the presence of intact virions. This may have practical implications for performing population-based analyses of disease prevalence and disease progression and have utility in assessing changes in viral replication that occur in response to antiviral or possibly immunomodulatory therapies for COVID-19 disease.

## ■ ASSOCIATED CONTENT

### SI Supporting Information

The Supporting Information is available free of charge at <https://pubs.acs.org/doi/10.1021/acs.jproteome.1c00391>.

Table S1. List of proteins identified from TMT 10-plex labeling-based quantitative proteomic analysis of 5 SARS-CoV-2 positive and 5 negative urine samples (XLSX)

Table S2. List of differentially abundant proteins identified from quantitative proteomic analysis of 5 SARS-CoV-2 positive and 5 negative urine samples (XLSX)

Table S3A. List of gene ontology terms enriched among the proteins with increased abundance in urine of SARS-CoV-2 positive individuals compared to negative individuals Table S3B. List of gene ontology terms enriched among the proteins with decreased abundance in urine of SARS-CoV-2 positive individuals compared to negative individuals (XLSX)

## ■ AUTHOR INFORMATION

### Corresponding Author

**Akhilesh Pandey** – Department of Laboratory Medicine and Pathology, Mayo Clinic, Rochester, Minnesota 55905, United States; Center for Molecular Medicine, National Institute of Mental Health and Neurosciences, Bangalore 560029, Karnataka, India; Center for Individualized Medicine, Mayo Clinic, Rochester, Minnesota 55905, United States; [orcid.org/0000-0001-9943-6127](https://orcid.org/0000-0001-9943-6127); Phone: 507-293-9564; Email: [pandey.akhilesh@mayo.edu](mailto:pandey.akhilesh@mayo.edu)

### Authors

**Sandip Chavan** – Department of Laboratory Medicine and Pathology, Mayo Clinic, Rochester, Minnesota 55905, United States

**Kiran K. Mangalparthi** – Department of Laboratory Medicine and Pathology, Mayo Clinic, Rochester, Minnesota 55905, United States

**Smrita Singh** – Department of Laboratory Medicine and Pathology, Mayo Clinic, Rochester, Minnesota 55905, United States; Institute of Bioinformatics, Bangalore 560066, Karnataka, India; Manipal Academy of Higher Education, Manipal 576104, Karnataka, India; Center for Molecular Medicine, National Institute of Mental Health and Neurosciences, Bangalore 560029, Karnataka, India

**Santosh Renuse** – Department of Laboratory Medicine and Pathology, Mayo Clinic, Rochester, Minnesota 55905, United States; Center for Individualized Medicine, Mayo Clinic, Rochester, Minnesota 55905, United States

**Patrick M. Vanderboom** – Department of Laboratory Medicine and Pathology, Mayo Clinic, Rochester, Minnesota 55905, United States

**Anil Kumar Madugundu** – Department of Laboratory Medicine and Pathology, Mayo Clinic, Rochester, Minnesota 55905, United States; Manipal Academy of Higher Education, Manipal 576104, Karnataka, India

**Rohit Budhraj** – Department of Laboratory Medicine and Pathology, Mayo Clinic, Rochester, Minnesota 55905, United States

**Kathrine McAulay** – Department of Laboratory Medicine and Pathology, Mayo Clinic, Phoenix, Arizona 85054, United States

**Thomas E. Grys** – Department of Laboratory Medicine and Pathology, Mayo Clinic, Phoenix, Arizona 85054, United States

**Andrew D. Rule** – Division of Nephrology and Hypertension, Department of Internal Medicine, Mayo Clinic, Rochester, Minnesota 55905, United States

**Mariam P. Alexander** – Division of Anatomic Pathology, Department of Laboratory Medicine and Pathology, Mayo Clinic, Rochester, Minnesota 55905, United States

**John C. O'Horo** – Division of Infectious Diseases, Department of Internal Medicine, Mayo Clinic, Rochester, Minnesota 55905, United States

**Andrew D. Badley** – Division of Infectious Diseases, Department of Internal Medicine, Mayo Clinic, Rochester, Minnesota 55905, United States

Complete contact information is available at:

<https://pubs.acs.org/10.1021/acs.jproteome.1c00391>

### Author Contributions

¶These authors contributed equally

### Funding

This study was supported by DBT/Wellcome Trust India Alliance Margdarshi Fellowship grant IA/M/15/1/502023 awarded to A.P. and the generosity of Eric and Wendy Schmidt. The sponsors had no role in the design and conduct of the study; collection, management, analysis, and interpretation of the data; preparation, review, or approval of the manuscript; or the decision to submit the manuscript for publication.

### Notes

The authors declare the following competing financial interest(s): A.D.B. is supported by grants from NIAID (grants AI110173 and AI120698), Amfar (#109593), and the Mayo Clinic (HH Shieck Khalifa Bib Zayed Al-Nahyan Named Professorship of Infectious Diseases). A.D.B. is a paid consultant for Abvie and Flambeau Diagnostics, a paid member of the DSMB for Corvus Pharmaceuticals, Equilibrium, and Excision Biotherapeutics; has received fees for speaking for Reach MD; owns equity for scientific advisory work in Zentalis and nference; and is the founder and President of Splissen therapeutics. T.E.G. is a consultant for Safe Health Systems, on the scientific advisory board of Dropworks and a founder of Cactus Bio, LLC. J.C.O. reports personal fees from Elsevier, Inc. and personal fees from EBates College, outside the submitted work. S.C., K.K.M., S.S., S.R., P.M.V., A.K.M., R.B., K.M., A.D.R., M.P.A., and A.P. have no conflicts of interest to declare.

### REFERENCES

- (1) WHO Coronavirus (COVID-19) Dashboard. <https://covid19.who.int/> (accessed May 24, 2021).
- (2) To, K. K.; Tsang, O. T.; Leung, W. S.; Tam, A. R.; Wu, T. C.; Lung, D. C.; Yip, C. C.; Cai, J. P.; Chan, J. M.; Chik, T. S.; Lau, D. P.; Choi, C. Y.; Chen, L. L.; Chan, W. M.; Chan, K. H.; Ip, J. D.; Ng, A. C.; Poon, R. W.; Luo, C. T.; Cheng, V. C.; Chan, J. F.; Hung, I. F.; Chen, Z.; Chen, H.; Yuen, K. Y. Temporal profiles of viral load in posterior oropharyngeal saliva samples and serum antibody responses during infection by SARS-CoV-2: an observational cohort study. *Lancet Infect. Dis.* **2020**, *20* (5), 565–574.
- (3) Wang, W.; Xu, Y.; Gao, R.; Lu, R.; Han, K.; Wu, G.; Tan, W. Detection of SARS-CoV-2 in Different Types of Clinical Specimens. *JAMA* **2020**, *323* (18), 1843–1844.
- (4) Xie, C.; Jiang, L.; Huang, G.; Pu, H.; Gong, B.; Lin, H.; Ma, S.; Chen, X.; Long, B.; Si, G.; Yu, H.; Jiang, L.; Yang, X.; Shi, Y.; Yang, Z. Comparison of different samples for 2019 novel coronavirus detection by nucleic acid amplification tests. *Int. J. Infect. Dis.* **2020**, *93*, 264–267.
- (5) Sun, J.; Zhu, A.; Li, H.; Zheng, K.; Zhuang, Z.; Chen, Z.; Shi, Y.; Zhang, Z.; Chen, S. B.; Liu, X.; Dai, J.; Li, X.; Huang, S.; Huang, X.; Luo, L.; Wen, L.; Zhuo, J.; Li, Y.; Wang, Y.; Zhang, L.; Zhang, Y.; Li, F.; Feng, L.; Chen, X.; Zhong, N.; Yang, Z.; Huang, J.; Zhao, J.; Li, Y. M. Isolation

of infectious SARS-CoV-2 from urine of a COVID-19 patient. *Emerging Microbes Infect.* **2020**, *9* (1), 991–993.

(6) Peng, L.; Liu, J.; Xu, W.; Luo, Q.; Chen, D.; Lei, Z.; Huang, Z.; Li, X.; Deng, K.; Lin, B.; Gao, Z. SARS-CoV-2 can be detected in urine, blood, anal swabs, and oropharyngeal swabs specimens. *J. Med. Virol.* **2020**, *92* (9), 1676–1680.

(7) Wang, L.; Li, X.; Chen, H.; Yan, S.; Li, D.; Li, Y.; Gong, Z. Coronavirus Disease 19 Infection Does Not Result in Acute Kidney Injury: An Analysis of 116 Hospitalized Patients from Wuhan, China. *Am. J. Nephrol.* **2020**, *51* (5), 343–348.

(8) Kuba, K.; Imai, Y.; Rao, S.; Gao, H.; Guo, F.; Guan, B.; Huan, Y.; Yang, P.; Zhang, Y.; Deng, W.; Bao, L.; Zhang, B.; Liu, G.; Wang, Z.; Chappell, M.; Liu, Y.; Zheng, D.; Leibbrandt, A.; Wada, T.; Slutsky, A. S.; Liu, D.; Qin, C.; Jiang, C.; Penninger, J. M. A crucial role of angiotensin converting enzyme 2 (ACE2) in SARS coronavirus-induced lung injury. *Nat. Med.* **2005**, *11* (8), 875–9.

(9) Zamorano Cuervo, N.; Grandvaux, N. ACE2: Evidence of role as entry receptor for SARS-CoV-2 and implications in comorbidities. *eLife* **2020**, *9*, e61390.

(10) Albini, A.; Di Guardo, G.; Noonan, D. M.; Lombardo, M. The SARS-CoV-2 receptor, ACE-2, is expressed on many different cell types: implications for ACE-inhibitor- and angiotensin II receptor blocker-based cardiovascular therapies. *Intern Emerg Med.* **2020**, *15* (5), 759–766.

(11) Bansal, M. Cardiovascular disease and COVID-19. *Diabetes Metab Syndr* **2020**, *14* (3), 247–250.

(12) Khawaja, S. A.; Mohan, P.; Jabbour, R.; Bampouri, T.; Bowsher, G.; Hassan, A. M. M.; Huq, F.; Baghdasaryan, L.; Wang, B.; Sethi, A.; Sen, S.; Petraco, R.; Ruparel, N.; Nijjer, S.; Malik, I.; Foale, R.; Bellamy, M.; Kooner, J.; Rana, B.; Cole, G.; Sutaria, N.; Kanaganayagam, G.; Nihoyannopoulos, P.; Fox, K.; Plymen, C.; Pabari, P.; Howard, L.; Davies, R.; Haji, G.; Lo Giudice, F.; Kanagaratnam, P.; Anderson, J.; Chukwumeka, A.; Khamis, R.; Varnava, A.; Baker, C. S. R.; Francis, D. P.; Asaria, P.; Al-Lamee, R.; Mikhail, G. W. COVID-19 and its impact on the cardiovascular system. *Open Heart* **2021**, *8* (1), e001472.

(13) Fotuhi, M.; Mian, A.; Meysami, S.; Raji, C. A. Neurobiology of COVID-19. *J. Alzheimer's Dis.* **2020**, *76* (1), 3–19.

(14) Jothimani, D.; Venugopal, R.; Abedin, M. F.; Kaliamoorthy, L.; Rela, M. COVID-19 and the liver. *J. Hepatol.* **2020**, *73* (5), 1231–1240.

(15) Wu, J.; Song, S.; Cao, H. C.; Li, L. J. Liver diseases in COVID-19: Etiology, treatment and prognosis. *World J. Gastroenterol* **2020**, *26* (19), 2286–2293.

(16) Gabarre, P.; Dumas, G.; Dupont, T.; Darmon, M.; Azoulay, E.; Zafrani, L. Acute kidney injury in critically ill patients with COVID-19. *Intensive Care Med.* **2020**, *46* (7), 1339–1348.

(17) Zhao, M.; Li, M.; Yang, Y.; Guo, Z.; Sun, Y.; Shao, C.; Li, M.; Sun, W.; Gao, Y. A comprehensive analysis and annotation of human normal urinary proteome. *Sci. Rep.* **2017**, *7* (1), 3024.

(18) Li, Y.; Wang, Y.; Liu, H.; Sun, W.; Ding, B.; Zhao, Y.; Chen, P.; Zhu, L.; Li, Z.; Li, N.; Chang, L.; Wang, H.; Bai, C.; Xu, P. Urine proteome of COVID-19 patients. *Urine (Amst)* **2020**, *2*, 1–8.

(19) Tian, W.; Zhang, N.; Jin, R.; Feng, Y.; Wang, S.; Gao, S.; Gao, R.; Wu, G.; Tian, D.; Tan, W.; Chen, Y.; Gao, G. F.; Wong, C. C. L. Immune suppression in the early stage of COVID-19 disease. *Nat. Commun.* **2020**, *11* (1), 5859.

(20) Doellinger, J.; Schneider, A.; Hoeller, M.; Lasch, P. Sample Preparation by Easy Extraction and Digestion (SPEED) - A Universal, Rapid, and Detergent-free Protocol for Proteomics Based on Acid Extraction. *Mol. Cell Proteomics* **2020**, *19* (1), 209–222.

(21) Sathe, G.; Na, C. H.; Renuse, S.; Madugundu, A. K.; Albert, M.; Moghekar, A.; Pandey, A. Quantitative Proteomic Profiling of Cerebrospinal Fluid to Identify Candidate Biomarkers for Alzheimer's Disease. *Proteomics: Clin. Appl.* **2019**, *13* (4), No. 1800105.

(22) Tyanova, S.; Temu, T.; Sinitcyn, P.; Carlson, A.; Hein, M. Y.; Geiger, T.; Mann, M.; Cox, J. The Perseus computational platform for comprehensive analysis of (prote)omics data. *Nat. Methods* **2016**, *13* (9), 731–40.

- (23) Huang, D. W.; Sherman, B. T.; Lempicki, R. A. Systematic and integrative analysis of large gene lists using DAVID bioinformatics resources. *Nat. Protoc.* **2009**, *4* (1), 44–57.
- (24) Szklarczyk, D.; Gable, A. L.; Lyon, D.; Junge, A.; Wyder, S.; Huerta-Cepas, J.; Simonovic, M.; Doncheva, N. T.; Morris, J. H.; Bork, P.; Jensen, L. J.; Mering, C. V. STRING v11: protein-protein association networks with increased coverage, supporting functional discovery in genome-wide experimental datasets. *Nucleic Acids Res.* **2019**, *47* (D1), D607–D613.
- (25) Tsukaguchi, H.; Sudhakar, A.; Le, T. C.; Nguyen, T.; Yao, J.; Schwimmer, J. A.; Schachter, A. D.; Poch, E.; Abreu, P. F.; Appel, G. B.; Pereira, A. B.; Kalluri, R.; Pollak, M. R. NPHS2 mutations in late-onset focal segmental glomerulosclerosis: R229Q is a common disease-associated allele. *J. Clin. Invest.* **2002**, *110* (11), 1659–66.
- (26) Boute, N.; Gribouval, O.; Roselli, S.; Benessy, F.; Lee, H.; Fuchshuber, A.; Dahan, K.; Gubler, M. C.; Niaudet, P.; Antignac, C. NPHS2, encoding the glomerular protein podocin, is mutated in autosomal recessive steroid-resistant nephrotic syndrome. *Nat. Genet.* **2000**, *24* (4), 349–54.
- (27) Cilia La Corte, A. L.; Carter, A. M.; Rice, G. I.; Duan, Q. L.; Rouleau, G. A.; Adam, A.; Grant, P. J.; Hooper, N. M. A functional XPNPEP2 promoter haplotype leads to reduced plasma aminopeptidase P and increased risk of ACE inhibitor-induced angioedema. *Hum. Mutat.* **2011**, *32* (11), 1326–31.
- (28) Venema, R. C.; Ju, H.; Zou, R.; Venema, V. J.; Ryan, J. W. Cloning and tissue distribution of human membrane-bound aminopeptidase P. *Biochim. Biophys. Acta, Gene Struct. Expression* **1997**, *1354* (1), 45–8.
- (29) Woodard-Grice, A. V.; Lucisano, A. C.; Byrd, J. B.; Stone, E. R.; Simmons, W. H.; Brown, N. J. Sex-dependent and race-dependent association of XPNPEP2 C-2399A polymorphism with angiotensin-converting enzyme inhibitor-associated angioedema. *Pharmacogenet. Genomics* **2010**, *20* (9), 532–6.
- (30) Duan, Q. L.; Nikpoor, B.; Dube, M. P.; Molinaro, G.; Meijer, I. A.; Dion, P.; Rochefort, D.; Saint-Onge, J.; Flury, L.; Brown, N. J.; Gainer, J. V.; Rouleau, J. L.; Agostoni, A.; Cugno, M.; Simon, P.; Clavel, P.; Potier, J.; Wehbe, B.; Benarbia, S.; Marc-Aurele, J.; Chanard, J.; Foroud, T.; Adam, A.; Rouleau, G. A. A variant in XPNPEP2 is associated with angioedema induced by angiotensin I-converting enzyme inhibitors. *Am. J. Hum. Genet.* **2005**, *77* (4), 617–26.
- (31) Broer, S.; Bailey, C. G.; Kowalczyk, S.; Ng, C.; Vanslambrouck, J. M.; Rodgers, H.; Auray-Blais, C.; Cavanaugh, J. A.; Broer, A.; Rasko, J. E. J. Iminoglycinuria and hyperglycinuria are discrete human phenotypes resulting from complex mutations in proline and glycine transporters. *J. Clin. Invest.* **2008**, *118* (12), 3881–3892.
- (32) Bermingham, J. R., Jr.; Pennington, J. Organization and expression of the SLC36 cluster of amino acid transporter genes. *Mamm. Genome* **2004**, *15* (2), 114–25.
- (33) Werion, A.; Belkhir, L.; Perrot, M.; Schmit, G.; Aydin, S.; Chen, Z.; Penaloza, A.; De Greef, J.; Yildiz, H.; Pothen, L.; Yombi, J. C.; Dewulf, J.; Scohy, A.; Gerard, L.; Wittebole, X.; Laterre, P.-F.; Miller, S. E.; Devuyt, O.; Jadoul, M.; Morelle, J.; Aboubakar, F.; Acid, S.; Amini, N.; Bailly, S.; Beauloye, C.; Castanares-Zapatero, D.; Coche, E.; Collienne, C.; Cornette, P.; De Brauwier, I.; Dechamps, M.; Dupriez, F.; Froidure, A.; Garnir, Q.; Gerber, B.; Ghaye, B.; Gilard, I.; Gohy, S.; Gregoire, C.; Hantson, P.; Jacquet, L.-M.; Kabamba, B.; Kautbally, S.; Lanthier, N.; Larbaoui, F.; Liistro, G.; Maes, F.; Montiel, V.; Mwenge, B.; Pierard, S.; Pilette, C.; Pouleur, A. C.; Sogorb, A.; Starkel, P.; Rodriguez-Villalobos, H.; Thoma, M.; Van Caeneghem, O.; Vancraeynest, D. SARS-CoV-2 causes a specific dysfunction of the kidney proximal tubule. *Kidney Int.* **2020**, *98* (5), 1296–1307.
- (34) Grempler, R.; Augustin, R.; Froehner, S.; Hildebrandt, T.; Simon, E.; Mark, M.; Eickelmann, P. Functional characterisation of human SGLT-5 as a novel kidney-specific sodium-dependent sugar transporter. *FEBS Lett.* **2012**, *586* (3), 248–53.
- (35) Wright, E. M.; Hirayama, B. A.; Loo, D. F. Active sugar transport in health and disease. *J. Intern. Med.* **2007**, *261* (1), 32–43.
- (36) Lin, Y.; Shen, X.; Yang, R. F.; Li, Y. X.; Ji, Y. Y.; He, Y. Y.; Shi, M. D.; Lu, W.; Shi, T. L.; Wang, J.; Wang, H. X.; Jiang, H. L.; Shen, J. H.; Xie, Y. H.; Wang, Y.; Pei, G.; Shen, B. F.; Wu, J. R.; Sun, B. Identification of an epitope of SARS-coronavirus nucleocapsid protein. *Cell Res.* **2003**, *13* (3), 141–5.
- (37) Bar-On, Y. M.; Flamholz, A.; Phillips, R.; Milo, R. SARS-CoV-2 (COVID-19) by the numbers. *eLife* **2020**, *9*, e57309.
- (38) Larsen, C. P.; Bourne, T. D.; Wilson, J. D.; Saqqa, O.; Sharshir, M. A. Collapsing Glomerulopathy in a Patient With COVID-19. *Kidney Int. Rep.* **2020**, *5* (6), 935–939.
- (39) Braun, F.; Lutgehetmann, M.; Pfefferle, S.; Wong, M. N.; Carsten, A.; Lindenmeyer, M. T.; Norz, D.; Heinrich, F.; Meissner, K.; Wichmann, D.; Kluge, S.; Gross, O.; Pueschel, K.; Schroder, A. S.; Edler, C.; Aepfelbacher, M.; Puelles, V. G.; Huber, T. B. SARS-CoV-2 renal tropism associates with acute kidney injury. *Lancet* **2020**, *396* (10251), 597–598.
- (40) Van Why, S. K.; Mann, A. S.; Ardito, T.; Siegel, N. J.; Kashgarian, M. Expression and molecular regulation of Na(+)-K(+)-ATPase after renal ischemia. *Am. J. Physiol.* **1994**, *267* (1), F75–F85.
- (41) Kwon, T. H.; Frokiaer, J.; Han, J. S.; Knepper, M. A.; Nielsen, S. Decreased abundance of major Na(+) transporters in kidneys of rats with ischemia-induced acute renal failure. *Am. J. Physiol. Renal Physiol* **2000**, *278* (6), F925–39.
- (42) Wang, Z.; Rabb, H.; Haq, M.; Shull, G. E.; Soleimani, M. A possible molecular basis of natriuresis during ischemic-reperfusion injury in the kidney. *J. Am. Soc. Nephrol.* **1998**, *9* (4), 605–13.
- (43) Li, D.; Zou, L.; Feng, Y.; Xu, G.; Gong, Y.; Zhao, G.; Ouyang, W.; Thurman, J. M.; Chao, W. Complement Factor B Production in Renal Tubular Cells and Its Role in Sodium Transporter Expression During Polymicrobial Sepsis. *Crit. Care Med.* **2016**, *44* (5), e289–99.